

USE OF PHOTOELASTICITY FOR VALIDATION OF NUMERIC MODELS

Braitner Lobato da Silva, lobatodecristo@yahoo.com.br.

Eduardo César Gavazza Menin, edumeni@unb.br.

University of Brasilia

Jorge Luiz de Almeida Ferreira, jorge@unb.br.

University of Brasilia

***Abstract.** The crescent progress of computation has generated a powerful and efficient model of numeric tools for the stress analysis. Though, because of their limitations, it lacks validation. The photoelasticity is an experimental tool based in an optic phenomena that comes to highlight the world scenery for its validation of numeric models. This work will make use of a plane with central hole to verify the use of the hybrid technique through the determination of the stress concentration factor. The study begins making the test body with photoelastic material: polycarbonate. After identification of residual stress existent caused by the production process, it was made a thermal treatment. Soon afterwards, the model was loaded. With intention of guaranteeing that the results was reliable, the fringe order in the border of the hole was determined 10 times. The second stage consisted of modeling the test body with the geometry of the previous model and submitting it to the same load conditions in the commercial package Ansys 5.2. The obtained results were expressive and satisfactory presenting an error less than 2%.*

Keywords: Photoelasticity Analysis, Numeric Models, Hybrid Method, Validation

1. INTRODUCTION

Projects of mechanical components demand the evaluation of structural flaws caused by the growth of trines close to areas of concentration of stresses. These projects also request isolated or combined use of numeric, analytical and experimental tools in way to obtain solutions that, in the point of view of the structural integrity, are safe and reliable (da Silva et al, 2006).

The analysis of stresses accomplished through analytical or computational techniques not always supply compatible answers with reality, because of idealizations and assumed simplifications. In these cases the experimental analysis of tensions becomes a quite effective project's tool.

The technological progress allowed a vast development in numeric methodologies. From there, the necessity of validation of those methods grew indeed with the intention to provide larger reliability to the results obtained by computational solutions and to verify how necessary the numeric models are. Among the experimental techniques available, Photoelasticity is one of the most versatile and it is distinguished for allowing the visualization of the fields of elastic stresses and the quantification of their intensities. Besides, it is distinguished because certain isotropic materials present double refraction index, or birefringence, when submitted to a certain mechanical loading (Dally and Riley, 1991).

When these materials are observed under polarized light, a pattern of fringes appears as a series of colored or monochrome strips. Each strip represents a birefringence degree, corresponding to the stress and deformation states of the material in that point. Thus, the fringe pattern can be read as a topographical map of the distribution of stresses and deformations along the analyzed surface.

Thus, the distribution of stresses in the points of interest can be interpreted by the evaluation of the order of the local isochromatic fringe. Working in the elastic regime and interrupted the applied effort, the deformations are diminished and the structure of the material returns to the initial situation (Frocht, 1941).

The combined use of the numeric and experimental tools has intensified with the modelling through finite elements and its comparison with photoelasticity. The modernization of data acquisition accentuated the optic methods among the experimental procedures for the synergy with computational methodologies.

2. THEORETICAL FOUNDATIONS

2.1. Photoelasticity

The photoelasticity is a very versatile and necessary experimental method in the determination of the distribution of elastic stress in a body submitted to mechanical shipments. The description and understanding of optic phenomena is of fundamental importance in this analysis for it is based in the alterations of the behavior of the light when crossing a submitted transparent body to tensions inside of the elastic lineal domain.

2.1.1. Propagation of the light in isotropic and anisotropic materials

The optically isotropic substances are those that present the property of transmitting light waves with equal speed in all directions. As examples, water and some polymers without deformations can be mentioned. Anisotropic substances are those which have the property of transmitting the light with speed that depends on the propagation direction. Crystals, stresses glasses and some polymers have this property. If a light source was put in the center of a crystal block, one would observe that two different sets of waves would be irradiated outside of the block. For each incident ray, there are two emerging rays and one of them crosses the crystal block faster than the other. This leads to the peculiar effect known as double refraction or birefringence.

After the two wave fronts emerge from the plate, they will keep their paths so that the distance among them, known as relative retard, will stay constant. The lineal relative retard (R) depends evidently on the thickness of the plate and on the relative speed of light correspondent to the two wavelengths or, in other words, it depends on the difference between the refraction indexes. Therefore

$$R = (n_2 - n_1) \cdot h, \quad (1)$$

Where h represents the thickness of the plate and n_2 and n_1 are the refraction's indexes of the different wave components in the isotropic material.

In most of the photoelastic analyses, the phenomenon of the overlap of waves is mainly related to the width of the resulting wave. This is due to the fact that human eye and most of the optic instruments present an answer to the intensity of the light that is proportional to the square of the width of the resulting wave. The change in the luminous intensity through the phenomenon of the overlap of waves is known as luminous interference and it can be constructive or destructive. If the relative retard is exactly half of the wavelength, the two components will be exactly opposed each other. The valleys of one will coincide with the crests of the other, and they both will be annulled.

Beams of polarized light suffer interference only when their polarization azimuths are coincident. Therefore, although the light that emerges of a crystal plate usually consists of two polarized plan components which have a certain relative retard, the phenomenon of the interference won't be observed since the two components are polarized in perpendicular plans amongst themselves. If the components of the emerging plan polarized waves are brought to a common plan by the appropriate means, as it is done, the effects of the interference now can be observed.

2.1.2. Circular polariscope

Polariscope is optic instruments that use the properties of polarized light in its operations. In the experimental analysis of tensions, two arrangements frequently used are the plane polariscope and the circular polariscope. Their names are given according to the type of light used in the polariscope.

In both types, the light of the source is polarized by the first filter, known as polarizer. The second filter, the analyzer, can present its polarization axis forming an angle of 90° with the polarizer, so that any light polarized by the first filter will remain after the passage to the second. Two filters arranged like this are said "crossed" and the arrangement receives the name of dark field. If the analyzer axis is parallel to the polarizer axis, the arrangement is known as clear field.

In general, waves that cross a crystal plate divide themselves in two components that combine forming an elliptic polarized wave. If they present a relative retard of $\pi/2$, corresponding to the retard of a fourth of the wavelength, they will combine forming a wave polarized circularly. Crystals' plates that convert incident plan polarized waves in waves polarized circularly are known as quarter-wave plates. And instruments which have two quarter-wave plates put between the polarizer and the analyzer are known as circular polariscope.

The light is polarized circularly by the first quarter-wave plate and penetrates the object in study. The second quarter-wave plate is put with its polarization axis perpendicular polarization to the first, that is, the fast axis of the first plate aligned with the slow axis of the second. Thus, the second plate undoes the effect of the first. When the light circularly polarized by the first quarter-wave plate passes for a crystal sample, for instance, the light that emerges can be subdivided once again in two plan polarized components in right angles amongst themselves and in parallel directions to the polarizer axes of the sample. In polariscope with this assembly, the luminous intensity composes a known pattern of isochromatic fringes and it can be calculated as:

$$I = K \cdot \text{sen}^2\left(\frac{\Delta}{2}\right), \quad (2)$$

Where $k = a \cdot \cos(\alpha)$ and Δ is the relative phase retard among the two resulting waves.

Thus:

$$\Delta = \frac{2\pi \cdot h}{\lambda} (n_2 - n_1) \quad (3)$$

If we change the monochrome light by white light then, any light wave whose wavelength is the same – or multiple – of the relative delay will be extinguished by interference. When the relative retard increases progressively from zero, all the colors of the spectrum will be extinguished in shifts, beginning from the smallest wavelengths.

2.1.3. Relations between stress and optics

In 1853, Maxwell noticed that the changes in the refraction indexes were lineally proportional to the applied loads and consequently to the tensions and deformations to lineally elastic materials, according to the following relations:

$$\begin{aligned} n_1 - n_0 &= c_1 \cdot \sigma_1 + c_2 \cdot (\sigma_2 + \sigma_3), \\ n_2 - n_0 &= c_1 \cdot \sigma_2 + c_2 \cdot (\sigma_3 + \sigma_1), \\ n_3 - n_0 &= c_1 \cdot \sigma_3 + c_2 \cdot (\sigma_1 + \sigma_2), \end{aligned} \quad (4)$$

where σ_i represents the main tensions in a point; n_0 , the refractive index of the unloaded material; n_i , the indexes of refraction of the materials, under load application, associated with the directions of the main tensions; c_1 and c_2 , constants known as stress optic coefficients.

These equations affirm that the state of stresses in a point can be completely determined by means of the knowledge of the refractive indexes associated with the three main directions and the directions of the material's optic axes. In cases of plane stresses and using the relative changes in the refractive indexes, instead of the absolute ones, the index of refraction of the unloaded material can be eliminated and the following expression is obtained:

$$n_2 - n_1 = (c_2 - c_1) \cdot (\sigma_2 - \sigma_1) = c \cdot (\sigma_2 - \sigma_1), \quad (5)$$

Where "c" represents the relative stress optic coefficient. Its unit is called Brewster (1Brewster = 10^{-13} cm²/dina).

If a plate of photoelastic material is put in a polariscope, it acts like a uniaxial crystal, and its optic axes are parallel to the plate surface. Generally, a polarized plane wave that enters in the plate is divided in two components in the directions of the main stresses in the incidence point. As in the case of natural crystals, these components are transmitted with different speeds, so that when they emerge of the plate, they present a relative retard whose magnitude is directly proportional to the difference of main stresses. Also proportional to the thickness of the plate, we can express them by the equation:

$$\delta = h \cdot (n_2 - n_1) = c \cdot (\sigma_2 - \sigma_1) \cdot h \quad (6)$$

In a plane state of stresses, the relative phase retard (Δ) correspondent to the relative retard "R" between the two resulting waves is expressed as:

$$\Delta_{12} = \frac{2\pi \cdot h \cdot c}{\lambda} (\sigma_1 - \sigma_2) \quad (7)$$

As Brewster is not a unit used frequently in engineering, we can put the expression above in the following form:

$$(\sigma_1 - \sigma_2) = \frac{N \cdot f_\sigma}{h} \text{ N/m}^2, \quad (8)$$

$$\text{Where } N = \frac{\Delta}{2\pi}, \quad (9)$$

N represents the Fringe Order (relative retardation in terms of complete wave cycles, 2π); K represents a property of the material for a given wavelength known as fringe value for the material or coefficient stress-fringe and h , the thickness of the test body.

2.1.4. Spectrum of isochromatics

Let us suppose now that a test body of photoelastic material is put in one circular polariscope with arrangement of dark field, and is subjected to a gradually growing traction tension. When the body is not under tension, the material is isotropic and the field of the polariscope keeps dark. With the load application, the material becomes birefringent. With the use of white light and by means of load application, the image of the body appears colored.

When a small stress is applied in the test body, the retard is smaller than the wavelength of the smaller wave of visible light and all the colors of the spectrum are transmitted by the analyzer. Then the body appears white. With the tension's and retard's increase, each color of the luminous spectrum is extinguished. The model then displays the sequence of colors that results of the combination of the complementary colors of those extinguished by interference.

2.1.5. Technique of Compensation

The point-to-point determination of the isochromatic fringe orders requests that compensation techniques be used for determination of the fractional values of the fringe orders. The compensation method of Tardy is a relatively fast and simple technique and needs measurements of fractional fringe orders. The basic principle predicts that when the polarizer and the analyzer are aligned with the main directions and the quarter wave plates form an angle of 45°, a rotation of an angle, in the clockwise of the analyzer, will do the fringe order N to move for a position where the fringe order will be:

$$N = n + \frac{\lambda}{180^\circ} \quad (10)$$

When the retard reaches two wave cycles, the colors correspondent to the second order fringes which are not equal to the ones of the first will appear, because it can happen the simultaneous extinction of more than a color. But the fringes of third level and up consist especially of the colors pink and green, each time more pale in the high orders, on account of the interference of turning more and more complex.

2.2. Finite Element Method

The methodology used in Finite Elements is based in the polynomial interpolation of the elements that constitute its composition. The field of stresses, for instance, is given by the interpolation of the resulting values of the field of stresses in each node of the structure. The sum will have so many polynomial expressions as elements that resulted in the evaluation of the field in all the structure.

Through the minimization of functions, the values of the field in the nodes can be obtained. This process produces series of concomitant algebraic equations for the field values in each node. The numeric resolution for finite elements involves matrix manipulation, resolution of equations and numeric integration, routine procedures solved with the use of computers.

A finite elements program is constituted by three modules: the pre-processor, the processor and the post-processor. The pre-processor generates the geometry of the piece and imposes the outline conditions. The processor makes the analysis and selects the exit data that will be visualized in the post-processor.

The term 2D solid is used to identify a two-dimensional solid without restrictions of form, loading, material properties or outline conditions. The field of displacements involves the components u and v . The typical elements used in 2D solids are the triangles and the squares with three degrees of translation freedom for node (Cook, 1994).

Adopting the notation used by Cook, it can be considered $u=u(x, y)$, $v=v(x, y)$ and $w=w(x, y)$ as the components of the displacements of an arbitrary point in the solids in the directions x and y , and if the stresses and the rotations are small, one can link the efforts and their gradients through the equations:

$$\varepsilon_x = \frac{\partial u}{\partial x}; \varepsilon_y = \frac{\partial v}{\partial y}; \gamma_{xy} = \frac{\partial u}{\partial y} + \frac{\partial v}{\partial x} \quad (11)$$

The equations can also be written in matrix form:

$$\begin{Bmatrix} \varepsilon_x \\ \varepsilon_y \\ \gamma_{xy} \end{Bmatrix} = \begin{bmatrix} \partial/\partial x & 0 \\ 0 & \partial/\partial y \\ \partial/\partial y & \partial/\partial x \end{bmatrix} \begin{Bmatrix} u \\ v \end{Bmatrix}; \text{ or } \varepsilon = \partial u. \quad (12)$$

The displacements \mathbf{u} in a plan of finite elements are interpolated starting from the displacements in nodes u_i and v_i in the usual way, meaning $\mathbf{u}=\mathbf{N}\mathbf{d}$. If the nodes only have degrees of translation freedom and n is the number of nodes by element, the matrix form of function \mathbf{N} has $2n$ columns for an element 2D, thus, for 2D solids, where $\mathbf{u}=\mathbf{N}\mathbf{d}$:

$$\begin{Bmatrix} u \\ v \end{Bmatrix} = \begin{bmatrix} N_1 & 0 & N_2 & 0 & \dots \\ 0 & N_1 & 0 & N_{21} & \dots \end{bmatrix} \begin{Bmatrix} u_1 \\ v_1 \\ u_2 \\ v_2 \\ \vdots \end{Bmatrix} \quad (13)$$

Making the $\mathbf{u}=\mathbf{N}\mathbf{d}$ substitution in the stress-deformation relation it is obtained the stress-deformation matrix \mathbf{B} , that enters in the formula of the integrating to the calculation of the rigidity matrix \mathbf{k} of the element.

$$\boldsymbol{\varepsilon} = \partial \mathbf{N}\mathbf{d}, \text{ or } \boldsymbol{\varepsilon} = \mathbf{B}\mathbf{d}, \text{ where } \mathbf{B} = \partial \mathbf{N} \quad (14)$$

A general formula for the calculation of \mathbf{k} is obtained by deriving an expression for U_0 , the deformation energy by unit of volume in an elastic material. In the matrix format and in terms of the deformation this expression is: $U_0 = \boldsymbol{\varepsilon}^T E \boldsymbol{\varepsilon} / 2$. Integrating the expression on a volume, V , and substituting in Eq. (15), it is obtained an element of deformation energy (Cook, 1994):

$$U = \frac{1}{2} \int \boldsymbol{\varepsilon}^T E \boldsymbol{\varepsilon} dV = \frac{1}{2} d^T \int \mathbf{B}^T E \mathbf{B} dV d = \frac{1}{2} d^T \mathbf{k} d \quad (15)$$

An expression for the rigidity matrix \mathbf{k} can be identified in Eq.(15) which can be applied to all finite elements problems based on displacements.

$$\mathbf{k} = \int \mathbf{B}^T E \mathbf{B} dV \quad (16)$$

3. METHODS

3.1. Experimental

The selected geometry is very frequent in machines and structural components. The study of distribution and concentration mechanisms of stresses and deformations in the proximity of the incisions are of great interest for the engineering. The selected material for the analysis, polycarbonate, PSM-01, with fringe value equal to 7002 Pa/fr.m, will be evaluated for monotonic loading conditions.

Initially the models were arranged in the circular polariscope, model P-150 of Riken Keiki Fine Instruments CO, and in one analysis of dark field the presence of residual tensions was verified. In order to eliminate them, they suffered relief in oven, model P-2307-M for photoelastics works, submitted to 250 °C for 24 hours.

After the preparation of the arrangement of the polarizer for one analysis of dark field, the material was *axially* loaded with 152.1 N. The calibration was made by rotation of the analyzer through displacement of the fringe of order 0 until a section presenting uniform tension. With the repetition of this procedure for the same loading, the reliability of the value obtained for the fringe was increased.

The point-to-point determination of isochromatic fringe orders requests that compensation techniques be used for the determination of the fractionary fringe order values. In the present work the method of compensation of Tardy was used. This procedure seeks the determination of the fractional value of the fringe order in the border of the hole. With this purpose, a load of 200.1 N was properly applied to the proof body in the circular polarizer prepared for one analysis of dark field. It has been made a division of the projected image in the screen in an appropriate number of points.

The procedure continued with the turn of the analyzer, making that the fringe of whole order N , visually recognized, coincide with the first point of interest. For the reading of the rotation of the analyzer, it becomes possible to determine the order of fractionary fringe of that point. With the attainment of this data for the several selected points, it will be possible the construction of a curve of the Order of fringe N versus the Location of the point. Through extrapolation of the curve it is obtained the order of fractionary fringe for the root of the incision and it becomes possible to determine the main stress in the border of the hole and also the theoretical stress concentration factor for the elastic regime.

3.2. Numeric

The commercial program ANSYS 5.2 was used to generate a discrete mesh from isoparametric triangular elements of constant deformation. All with six nodes for element and two degrees of freedom for node, according to Fig.(1). A fine mesh with 0.1 degrees was obtained possessing 20012 elements and 43774 nodes.

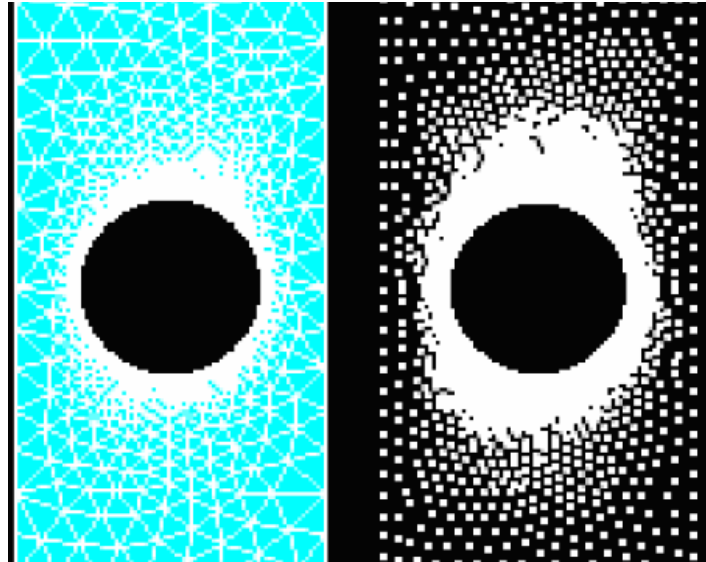


Figure 1. Mesh and nodes

4. RESULTS

4.1. Experimental results

The Figure (2) shows the curve obtained from the data of the Tab. (1). It relates the fringe order and the distance from the border of the hole of the projected image. Through the obtained graphic for the tendency equations, the extrapolation was done for the chosen point. The Table (2) introduces an order of medium fringe of 3.393 for the three experiments. The factor of sensibility used correspond to 6991 Pa/fr.m, in agreement with da Silva, 2006. Therefore, the result to the fringe order in the hole border was $3,39 \pm 0.01$.

The nominal stress is equal to 1.74 MPa. The maximum stress from the photoelastic test given by Eq. (8) is equal to 3.74 MPa. Therefore, from Eq. (3), the medium stress concentration factor is 2.123. The Figure (3) illustrates the fringe orders pattern in the identification of K_t .

Table 1. Experimental data obtained from the fringe order in the border of the hole.

	Experiment 1		Experiment 2		Experiment 3	
	Points (mm)	N	Points (mm)	N	Points (mm)	N
1	0	x	0	x	0	x
2	1	3.00	2	3.00	2	3.00
3	3	2.42	4	2.42	4	2.42
4	4	2.25	5	2.25	5	2.25
5	5	2.00	6	2.00	6	2.00
6	9	1.50	10	1.00	9	1.50
7	10	1.42	11	1.42	10	1.42
8	11	1.25	13	1.25	12	1.25
9	14	1.00	15	1.00	15	1.00

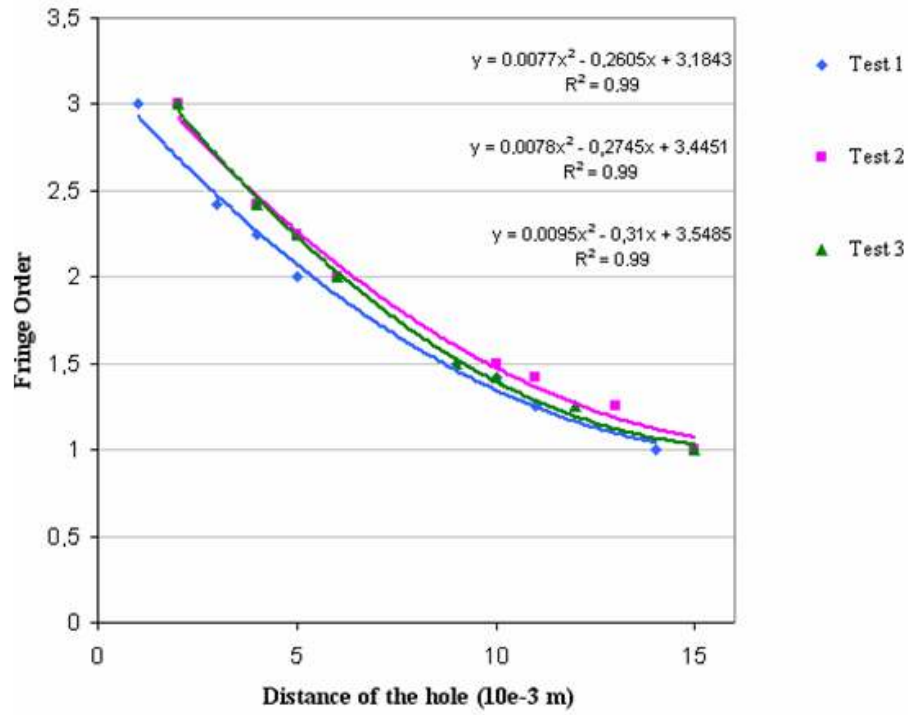


Figure 2. Relation between the fringe order and the distance of the hole for the projected image.

Table 2. Results of the extrapolation for the fringe order in the border of the hole.

Ensaio	N	\bar{N}	σ_N	σ_N (%)
1	3.184	3.393	0.188	0.055
2	3.445			
3	3.549			

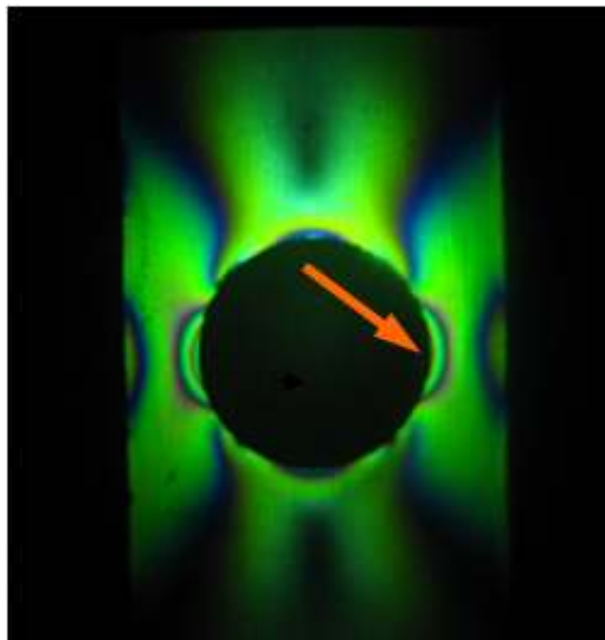


Figure3. Plane plate with central hole under shipment of 201.1 N

4.2. Numeric results

The numeric stress concentration factor is equal to 2.12. It was obtained from 20012 elements and 43774 nodes, according with Fig. (4). The analysis of convergence of the results can be seen in the Fig. (5) and the distribution of the ratio of the maximum stress for the normal stress along the axis y in the Fig.(6).

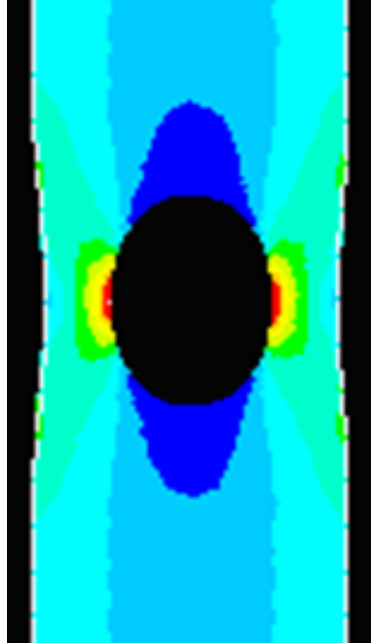


Figura 4. Stress distribution.

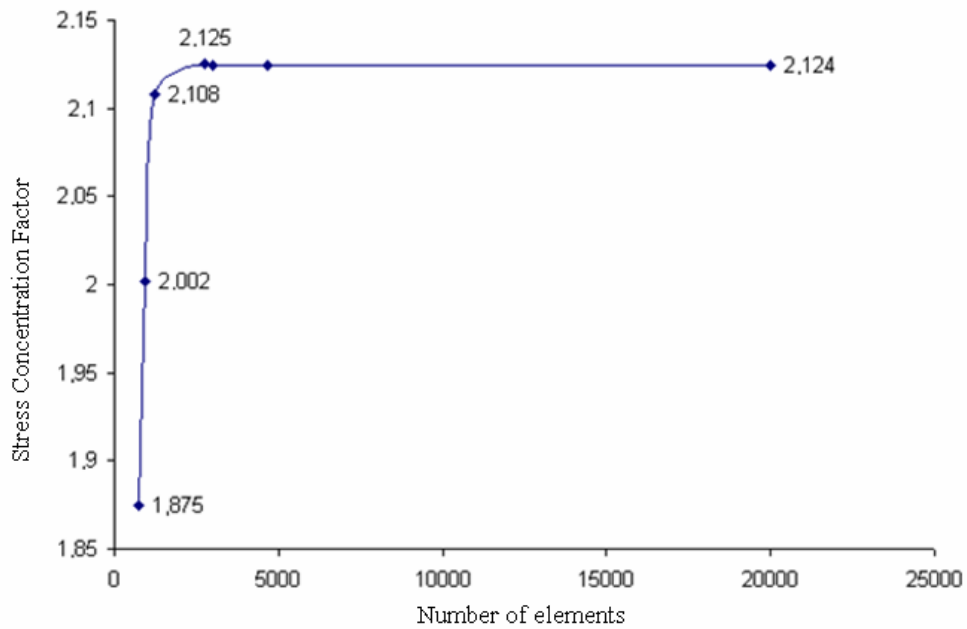


Figure 5. Convergence graph- Stress concentration - K_t

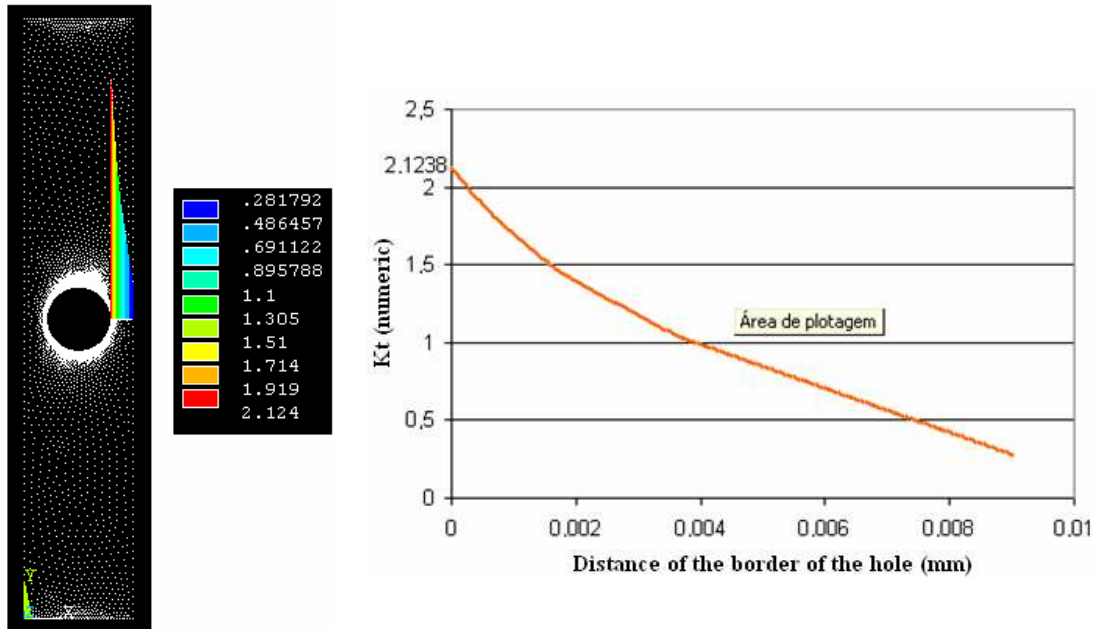


Figure 6. Distribution of the ratio of the maximum tension for the normal stress along the axis y.

5. CONCLUSION

The use of the photoelasticity is of great utility in the validation of numeric methods. The practical experimental methodology can be used with efficiency in the relief of practical problems in engineering. Though, we suggest the use of the digital photoelasticity in order to minimize the doubts associated to the analogical tests. However, the adopted hybrid technique presented satisfactory results concerning the deviation of results between finite elements and photoelasticity by transmission. This deviation was from centesimal order, less than 2%. It shows the importance of photoelasticity like a reliable tool in the validation of numeric methods.

6. ACKNOWLEDGEMENTS

We thank God for the gift of life and for the health. To GAMMA, Group of Solid Mechanic of the University of Brasília for the released support and to CNPq for the sponsorship.

7. REFERENCES

- Da Silva, B. L., 2006, "Calibração de Modelos Numéricos através da Fotoelasticidade", Report submitted as partial requirement for obtaining of Mechanical Engineer's degree of University of Brasília. Brasília, Brazil.
- Cook, Robert D., 1994, "Finite Element Modeling for Stress Analysis", John Wiley & Sons, Inc, New York.
- Dally, J.W., Riley, W. F., 1991, "Experimental Stress Analysis", 3rd ed, McGraw-Hill International Editions, New York, 639p.
- Frocht, M. M., 1941, "Photoelasticity", Vol. 1 e 2, John Willey & Sons, Inc., New York.
- Hendry, A. W., "Photoelastic Anallysis", Pergamon Press, Londres, 1966.
- Norton, R. L., "Projeto de Máquinas: uma abordagem integrada", 2 ed, Bookman, Porto Alegre.

8. RESPONSIBILITY NOTICE

The authors are the only responsible for the printed material included in this paper.